Numerical Analysis of the Pullout Bearing Characteristics of Artificial Excavated Piles with Post-Grouting after Prefabricated Retaining Walls

Lulu Wang[1], Jianbo Wang[2], Hanqin Wu[1], Jianxin Bao[2], Liming Yin[1], Xinjun Gao[2*]

[1]PowerChina Henan Electric Power Survey & Design Institute Co., Ltd., Zhengzhou, China
[2]School of Civil Engineering, Zhengzhou University, Zhengzhou, 450001, China

*Corresponding author: gxjun@zzu.edu.cn

Abstract. Precast retaining wall post-grouting manual excavation pile is a new type of pile foundation. It adopts the method of manual segmented excavation, installation of precast retaining wall to form holes and then pouring concrete and combined with the method of pressure grouting at the bottom of the pile, which overcomes the disadvantages of traditional cast-in-place retaining wall manual excavation pile, such as complicated process, long construction period, difficult to guarantee bearing capacity and high safety risk. However, up to now, the research on the key construction technology, bearing capacity and design theory of this pile type is still insufficient, which hinders the promotion and application of this technology to a certain extent. In order to investigate the pullout bearing characteristics of artificial excavated piles with post-grouting after prefabricated retaining walls, three-dimensional numerical models of two types of pullout piles—one with post-grouting and one without—were developed based on numerical methods. By comparing the calculations, the pullout characteristics of the post-grouted artificial excavated piles were revealed. The results indicate that post-grouting significantly enhances the ultimate pullout bearing capacity of the piles and reduces the uplift displacement; under the pressure of the grout, the infiltrating and compacting effect of the grout can more effectively transfer the load to the surrounding soil layers, significantly increasing the lateral resistance of the post-grouted piles compared to non-grouted piles. The failure mode of the post-grouted artificial excavated piles is characterized by cylindrical shear failure at the pile-soil interface. The research results provide a theoretical basis for the pullout design of artificial excavated piles with post-grouting after prefabricated retaining walls.

Keywords: Precast retaining wall bored pile; Post-grouting; Vertical uplift bearing capacity; Lateral resistance; Numerical simulation

1 Introduce

In recent years, with the continuous increase in voltage levels of transmission lines and the ongoing optimization of foundation design, excavation-type foundations that

Y. Zhang et al. (eds.), *Proceedings of the 2024 10th International Conference on Architectural, Civil and Hydraulic Engineering (ICACHE 2024)*, Advances in Engineering Research 259,
https://doi.org/10.2991/978-94-6463-658-1_60

can fully utilize the properties of undisturbed soil and are economically and environmentally friendly have gradually become the dominant choice for transmission tower foundations. Particularly in hilly and mountainous areas where the groundwater level is deep and access is limited for construction machinery, the application of artificial excavated piles is especially common, providing strong support for the smooth progress of transmission line projects[1]. Numerous scholars both domestically and internationally have conducted extensive research on the pullout bearing characteristics of these piles.

Turner[2] conducted research on the design criteria for artificial foundations of transmission towers under uplift load in the Houston Lighting & Power Company system using indoor models and field tests. They proposed design methods and calculation formulas for the uplift bearing capacity of transmission tower foundations. Imano[3] analyzed and summarized the experimental results regarding the pullout capacity of pile foundations installed on weathered rock by Tokyo Electric Power Company, studying the bearing mechanisms and influencing factors of transmission line tower foundations on weathered rock. Zhou[4] conducted a large-scale field study on three types of bored piles-rotary drilling piles, impact drilling piles, and artificial excavated piles. They pointed out that under the same conditions, the bearing capacity of artificial excavated piles is greater than that of the other two types, attributed to the minimal disturbance to the surrounding soil during the construction of artificial excavated piles and the relatively rough contact surface between the pile and soil, which enhances the lateral resistance of the pile. Zhang[5] studied the vertical load transfer characteristics of large-diameter rock-embedded artificial excavated piles based on load tests, indicating that the segmented excavation construction of the retaining wall creates repetitive disturbances in the soil with a superimposed effect, which may lead to cracks at the boundaries of the upper retaining wall under vertical load. Wang[6] used ANSYS software to establish shear and contact models for excavation foundations and explored the mechanical mechanisms of these two computational models under uplift force. Hao[7] simulated and analyzed the bearing behavior of excavated transmission tower foundations in undisturbed soil under uplift load using the finite element method, discussing the effects of parameters such as different burial depths and soil shear strength on the ultimate bearing capacity and failure modes of uplift piles through parametric analysis. Yu[8] studied the contribution of retaining structures to the vertical bearing capacity of the pile body using the finite element software ANSYS and further summarized a unified quantitative calculation formula for the contribution of the retaining wall to the vertical bearing capacity of the pile. Gao[9] investigated the mechanical characteristics of artificial excavated pile retaining walls at different excavation stages using ABAQUS, detailing the changes in bending moment, shear force, horizontal displacement, and the surface settlement curves of the surrounding soil of the pile as the construction progressed, and summarized factors affecting the working mechanism of artificial excavated pile retaining walls, including surrounding soil parameters, pile stiffness, and excavation depth per section. Lv[10] established a three-dimensional model considering pile-soil interaction using ABAQUS to study the pullout bearing characteristics of excavated piles for transmission line towers, analyzing in-depth the influence of structural parameters of the pile and soil properties on the uplift bearing capacity. In addition, some scholars have conducted in-depth research on this aspect and obtained a series of conclusions[11-14].

The above research provides a theoretical and practical foundation for the design and construction of artificial cast-in-situ retaining wall excavated piles. However, most current artificial excavated pile foundations use cast-in-situ reinforced concrete retaining walls, which have many shortcomings, including complex procedures, long construction periods, difficulties in ensuring bearing capacity, and high safety risks. Based on the above problem, this paper proposes a novel pile foundation form of artificial excavated piles with post-grouting and prefabricated retaining walls. This method involves artificial segmented excavation, the installation of prefabricated retaining walls, followed by concrete pouring and combined with pressure grouting at the pile bottom, effectively overcoming the disadvantages of traditional cast-in-situ retaining wall artificial excavated piles. Nevertheless, as a new type of pile, research on key construction techniques, bearing performance, and design theories remains insufficient, which hinders the promotion and application of this technology to some extent.

From the above, domestic and foreign scholars have systematically studied the construction method, bearing capacity of artificial cast-in-place wall protection dug pile and the influence of different post-grouting methods on the ultimate bearing capacity of the pile by combining field test and model test. However, this paper proposes a new type of pile foundation with prefabricated wall protection and artificial hole digging by grouting, which adopts the method of artificial section excavation and installation of prefabricated wall protection to make holes, and then concrete pouring combined with the method of pressure grouting at the bottom of the pile for construction. For this new pile type, the research on its uplift bearing characteristics is still in the initial stage. Due to the lack of research, the application of prefabricated post-wall grouting pile in transmission line engineering has not been widely popularized and practiced. Therefore, it is urgent to deepen the research on the anti-pull-bearing characteristics of prefabricated post-wall grouting pile, so as to provide a strong basis for its application in transmission line engineering. Therefore, this paper takes a segment of artificial excavated piles from the Hami-Chongqing ±800kV UHVDC transmission project as the research object, and based on numerical simulation, studies the load transfer mechanism of this new type of uplift pile. The findings are of significant engineering practical importance and profound theoretical implications for improving the uplift design methods of artificial excavated piles under prefabricated retaining wall construction conditions.

2 Engineering Background

The Hami-Chongqing ±800kV ultra-high voltage direct current transmission project is proposed to have its starting point to the north of Niwangbao Village, Anzi Town, Langzhong City, and terminate to the southeast of Shuiquan Village, with a line length of 128km. The proposed line design includes precast casing concrete bored piles with post-grouting, with pile length of 10 meters, pile diameter of 1.0 meters, and pile body strength of C30, with uplift resistance as the controlling load. Post-grouting is carried out by pile bottom grouting, using Ordinary Portland cement PO 42.5, with a water-cement ratio of 0.55~0.6. The single pile grouting volume is 2.1 tons, the grouting pressure is 0.4MPa, and the grouting slurry returns to the pile top after grouting. The diameter of the inner ring of the precast casing for the artificial bored piles is 1000mm, with a vertical height of 500mm and a thickness of 60mm. Each ring of precast casing is divided into three sections, with the concrete strength grade being C50. The main geological condition for the line is silt loess, with a relatively deep groundwater level. The physical parameters of the soil and the precast casing artificial bored piles are listed in Table 1.

Table 1. Mechanical Parameters of Soil and Pile Foundation Materials

Structure Name	Density (kg/m^3)	Elastic Modulus (MPa)	Poisson's Ratio	Cohesion (kPa)	Internal Friction Angle (°)
Silty Clay	1850	26	0.32	20	12
Grouted Reinforcement	2000	120	0.25	60	35
Prefabricated Retaining Wall	2400	3.0×10^4	0.22	/	/
Artificial Excavated Pile	2400	3.0×10^4	0.20	/	/

3 Precast Casing Artificially Excavated Pile Static Load Test Numerical Simulation

3.1 Model Establishment

This paper adopts the finite element software ABAQUS and relies on the prefabricated wall protection manual dug ungrouting pile and grouting pile of the ±800kV UHVDC transmission project in Hami-Chongqing. The parameters are shown in Section 1 engineering background. The three-dimensional numerical models of 1 ungrouting pile and 1 grouting pile were established respectively, and the vertical pull-out numerical simulation analysis was carried out to reveal the variation law of the pull-out bearing capacity, axial force and lateral resistance of the artificially dug grouting pile after prefabricated wall protection, and their failure modes were analyzed.

The numerical model has dimensions of 25m in length, width, and height. The center of the pile hole and the top of the soil mass are both located at the origin of the coordinate axes. The grouted solidification around the pile is simplified to a hollow cylinder with an inner diameter of 1.32m and a wall thickness of 0.2m. The grouted solidification at the pile tip is simplified to a cylindrical body with a height of 0.3m. The entire model is divided into a total of 41696 grids, as shown in Figure 1. The constitutive models for the soil, excavated pile, and grouted solidification are adopted as Mohr-Coulomb, linear elastic, respectively. The interface between the pile body and the casing of the artificial excavated pile is defined with a tie constraint, and the outer surface of the grouted solidification is defined with a Surface to Surface contact. Normal constraints are set at the four sides and the bottom of the model, with the top surface being a free boundary. When the post-grouting construction simulation is not used, the pile tip and the pile side solidification are removed, and the rest is the same as above.

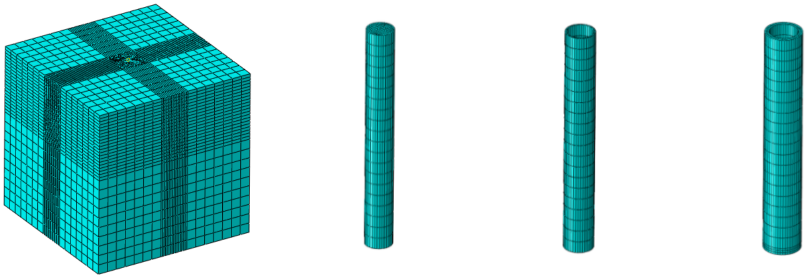

(a) Geometric Model and Mesh Division of Soil (b) Mesh Division of Pile Body (c) Mesh Division of Retaining Wall (d) Mesh Division of Grouted Body

Fig. 1. Model and Mesh Division of Prefabricated Retaining Wall and Artificial Excavated Pile

3.2 Numerical Analysis Department

Throughout the construction process, a total of 44 analysis steps were established. After the geo stress equilibrium analysis step, a step for the installation of precast casings on the retaining wall was added, followed by the add pile planting analysis step. Subsequently, the post-grouting analysis step was implemented, and finally, the load analysis step for the application of uplift load in graded increments was performed, as shown in Table 2.

Table 2. Finite Element Simulation Analysis Steps

No.	Analysis Step	Uplift Displacement at Pile Top (mm)
1	geo	/
2	retaining wall	/
3	addpile	/
4	post-grouting	/
5	Load-1	Step1
…	…	…
44	Load-40	Step40

4 Analysis of Numerical Simulation Results

4.1 Uplift Load-Displacement Curve Analysis

During the post-processing of the 3D model, the pile top load and uplift displacement data were extracted, and the uplift load-displacement curves for the non-grouted piles and the post-grouted piles were plotted, as shown in Figure 2.

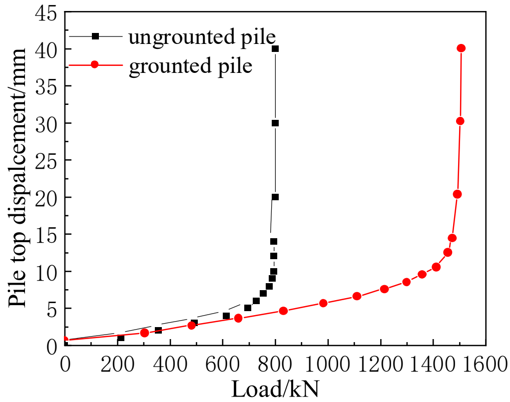

Fig. 2. Uplift Load-Displacement Curves of Ungrouted Piles and Grouted Piles

From Figure 2, it can be observed that the uplift load-displacement curves for both the non-grouted and the grouted piles exhibit a "sharp change" pattern. Initially, the displacement difference between the two pile types is small, but as the uplift load continues to increase, the displacement difference gradually becomes larger. During the application of the uplift load, the load-displacement curve of the grouted pile has a significantly lower slope compared to that of the non-grouted pile, and the displacement development at the pile top is relatively slow. Moreover, the load-displacement curve of the grouted pile is always located below and to the right of that of the non-grouted pile. The ultimate tensile bearing capacity of the non-grouted and grouted piles is 777kN and 1431kN, respectively, with the latter being approximately 84.17% higher than the former. Additionally, when the uplift force is around 777kN, the non-grouted pile reaches the ultimate tensile bearing state with a corresponding vertical displacement of 8mm, while the vertical displacement of the grouted pile is around 3.5mm, which is approximately 43.75% of the non-grouted pile. When the uplift force is around 1431kN, the grouted pile reaches the ultimate tensile bearing state with a corresponding vertical displacement of 10mm. Through the above comparative analysis, it can be seen that the grouted pile has a significant reduction in vertical displacement compared to the non-grouted pile, and the tensile bearing capacity is greatly improved. This indicates that the load transfer characteristics of the grouted pile have been significantly improved, and its tensile bearing capacity can be more fully utilized.

4.2 Pile Axial Force Analysis

Five groups from the 40 uplift displacement cases were selected to analyze the distribution pattern of the pile axial force along depth for both non-grouted and grouted piles. Specifically, the 5 uplift displacements for the non-grouted piles were 1 mm, 3mm, 5 mm, 8mm, and 20mm, while for the grouted piles, they were 1 mm, 3 mm, 5mm, 10mm, and 20mm. The distribution curves of the pile axial force for both non-grouted and grouted piles under different uplift displacements are shown in Figure 3.

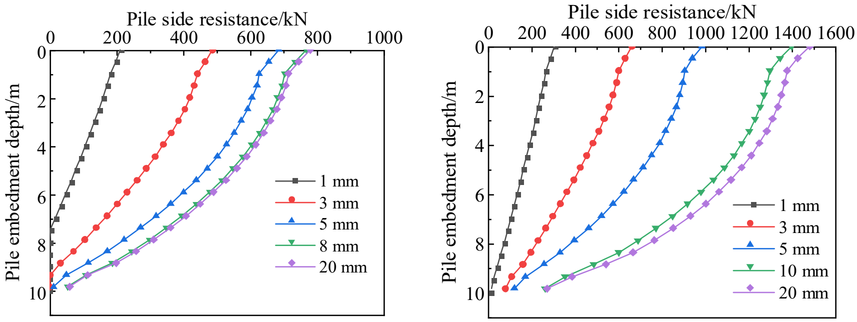

(a) Axial Force Distribution Curve of Ungrouted Pile(b) Axial Force Distribution Curve of Grouted Pile

Fig. 3. Axial Force Distribution Curves of Ungrouted and Grouted Piles at Different Uplift Displacements

From Figure 3, it is noted that the distribution curves of the pile axial force for the non-grouted pile and the grouted pile are similar. Under the action of various loads, the axial force at the same section increases with the increase of uplift load, and the increase in the magnitude of the axial force decreases gradually with the application of uplift load and tends to stabilize. Under the same level of load, the axial force at each section decreases gradually along the depth, which is due to the relative displacement between the pile top and soil under the uplift load, leading to the generation of pile side resistance. The pile side resistance is gradually exerted along the depth direction, and the axial force at the depth of the pile tip approaches zero. This indicates that the uplift force is borne by the side resistance of the pile section.

Comparative analysis of Figures (a) and (b) shows that under the same uplift load, the pile axial force at the same depth for the grouted piles is significantly greater than that for the non-grouted piles. For uplift displacements of 1mm, 3mm, and 5mm, the axial force at the top of the non-grouted pile is sequentially 214kN, 494kN, and 695kN, while for the grouted pile, it is 310kN, 670kN, and 997kN, respectively. The latter is 44.86%, 35.63%, and 43.46% greater than the former, respectively. Under the action of the grouting pressure, the grouting fluid, through the permeation and compaction effect, forms a grouting solidification zone within a certain range of the pile soil. The pile axial force of the artificial excavated pile, through the combined action with the grouting solidification zone, can transfer the load more effectively to the surrounding soil layer, thereby increasing the pile axial force of the post-grouted piles.

4.3 Pile Side Resistance Analysis

Figure 4 shows the distribution curves of pile side resistance for non-grouted piles and grouted piles under different uplift displacements.

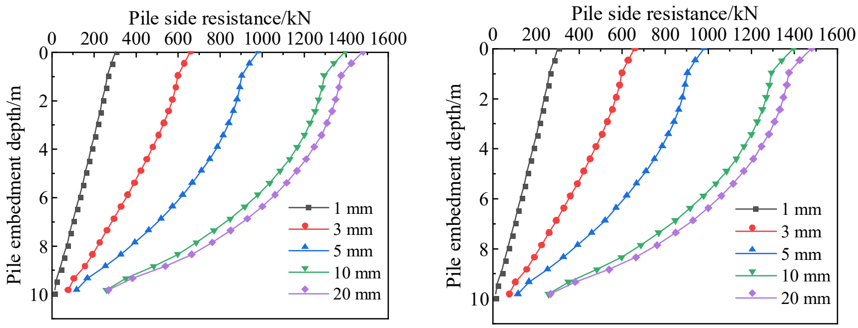

(a) Axial Force Distribution Curve of Ungrouted Pile(b) Axial Force Distribution Curve of Grouted Pile

Fig. 4. Side Resistance Distribution Curves of Ungrouted and Grouted Piles at Different Uplift Displacements

From Figure 4, it can be observed that the distribution curves of pile side resistance for both non-grouted and grouted piles show a similar pattern and exhibit an extremely nonlinear relationship. Under the same level of load, the pile side resistance at each section gradually increases along the burial depth direction, reaching a peak at a certain depth within the range of 0 to 1m of the pile body, and then attenuating to a certain value within the range of 1 to 2m. This is the phenomenon of side resistance softening, and then reaching the maximum peak of side resistance near the pile tip (within the range of 9 to 10 m of the pile body). This indicates that the pile side resistance is transmitted and exerted from top to bottom with increasing depth. By combining the distribution curves of pile side resistance from Figures (a) and (b), it is evident that under the same uplift load, the pile side resistance of grouted piles at the same depth is greater than that of non-grouted piles, suggesting that the post-grouted piles have a more fully developed pile side resistance compared to non-grouted piles. Under the ultimate load, the maximum pile side resistance for non-grouted piles is 42.25kPa, while for grouted piles, it is 72.56kPa, indicating an increase in pile side resistance of approximately 30% to 75%. This shows that the placement of grouting solidification material can transform the relatively smooth "concrete-soil" interaction interface of traditional artificial excavated piles into a "grouting material-soil" interaction interface. At this point, the pile side resistance changes from shear slip resistance to the bonding strength of the "grouting material-soil" interface. This allows the pile side resistance to be further fully utilized, thereby increasing the ultimate side resistance of the artificial excavated piles with post-grouted and prefabricated retaining walls.

4.4 Failure Mode Analysis

This study employed the PEEQ (Equivalent Plastic Strain) in ABAQUS software to investigate the failure mode of artificial excavated piles with post-grouting and pre-fabricated retaining walls. The distribution of the equivalent plastic strain region around the pile is shown in Figure 5.

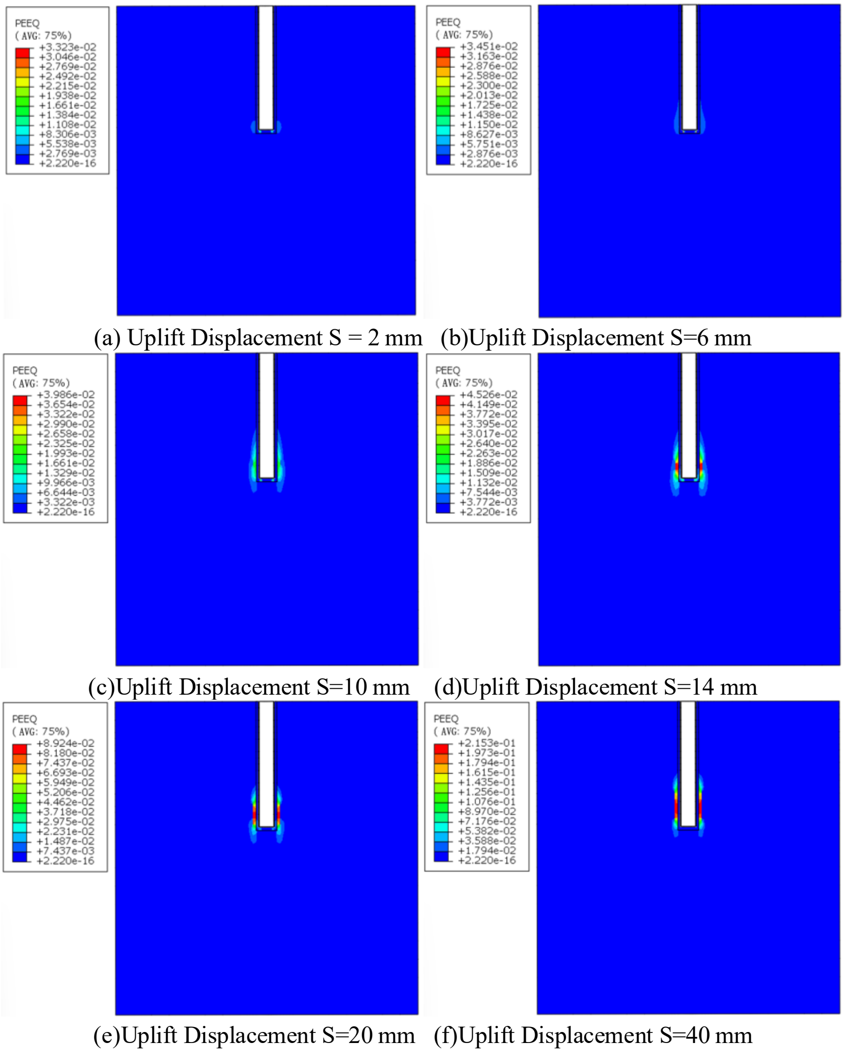

(a) Uplift Displacement S = 2 mm (b)Uplift Displacement S=6 mm

(c)Uplift Displacement S=10 mm (d)Uplift Displacement S=14 mm

(e)Uplift Displacement S=20 mm (f)Uplift Displacement S=40 mm

Fig. 5. Distribution of Equivalent Plastic Strain Areas around the Pile Soil

As can be seen from Figure 5, when the uplift displacement is relatively small (S=2mm), the soil around the lower part of the pile starts to exhibit characteristics of plastic yielding, indicating that a portion of the soil around the pile is beginning to undergo shear failure. As the uplift load increases gradually, the plastic area around the pile soil expands continuously, and the soil at the pile bottom also begins to experience plastic failure. With further increase in uplift load, the main failure zone of the artificial excavated piles with post-grouting and prefabricated retaining walls occurs in the lower part of the pile and between the grouted solidification zone directly contacting the soil at the bottom and the soil. The plastic deformation in these areas gradually intensifies, and the plastic zone gradually expands towards the pile top. When the ultimate load is reached (S=10mm), the soil around the pile and near the surface of the grouted solidification zone at the bottom of the pile both undergo severe shear failure. When the uplift displacement S reaches 40mm, the pile bottom completely detaches from the soil, forming a distinct separation state. From the above analysis, it can be concluded that the failure mode of artificial excavated piles with post-grouting and prefabricated retaining walls mainly manifests as cylindrical shear failure at the pile-soil interface.

5 Conclusion

In this paper, a finite element model is established by using ABAQUS finite element software, and the uplift bearing capacity of manually dug pile with prefabricated wall protection is compared and analyzed under two different conditions: ungrouting and grouting. The load-displacement curve analysis, pile axial force analysis, pile side resistance analysis, soil displacement change law around the pile and the development law of soil plastic zone around the pile are discussed. The influence mechanism of different post-grouting parameters on uplift bearing capacity is deeply analyzed, which provides an important theoretical basis and practical guidance for the design and construction of prefabricated post-grouting pile in HV transmission line engineering. This innovation not only simplifies the construction process and improves work efficiency, but also injects new vitality into the safety and economy of transmission line engineering. The main conclusions are as follows:

1)The load-displacement curve of the grouted piles is located in the lower right of the non-grouted piles, indicating that under the same load, the grouted piles have a smaller vertical displacement at the pile top. Moreover, the grouted piles have an 84.17% increase compared to the non-grouted piles, showing that post-grouting significantly improves the ultimate pullout bearing capacity of the piles and can reduce the uplift displacement.

2)The axial force of the piles, both in the non-grouted and grouted piles, decreases gradually with depth. However, under the action of the grouting pressure, the grouting fluid forms a grouted solidification zone around the pile within a certain range through the permeation and compaction effect. The axial force of the artificial excavated piles is transferred more effectively to the surrounding soil through the combined action with the grouted solidification zone, thereby increasing the axial force of the grouted piles.

3)The change of the pile side resistance along the burial depth direction for both non-grouted and grouted piles is nonlinear. The pile side resistance starts to operate from the upper part of the pile and gradually transmits downwards with the increase of uplift load, reaching a maximum near the pile tip. Under the ultimate load, the maximum pile side resistance for the non-grouted and grouted piles is 42.2kPa and 72.56kPa, respectively. After post-grouting, the pile side resistance increases by about 30% to 75%.

4)The prefabricated retaining wall grouted artificial excavated piles resist uplift loads through the larger pile side resistance between the grouted solidification zones at the pile sides and bottom and the soil. The failure mode is cylindrical shear failure at the pile-soil interface.

References

1. Mozakka I, Zeynalian M, Hashemi M. A feasibility study on construction methods of high voltage transmission towers' foundations[J]. Archives of Civil and Mechanical Engineering, 2021,21(2):1-15.
2. Turner E A, ASCE A M. Uplift Resistance of Transmission Tower Footings[J]. Journal of the Power Division, 1956,88(2):17-33.
3. Imano K. Bearing capacity of power transmission line tower foundation installed on weathered rock: Proceedings of the International Symposium on Weak Roc, Tokyo, Japan, 1981[C].
4. Zhou Z, Yang T, Fan H. A Full-Scale Field Study on Bearing Characteristics of Cast-in-Place Piles with Different Hole-Forming Methods in Loess Area[J]. Advances in Civil Engineering, 2019,2019:1-12.
5. Zhang Junjian, Sui Qianqian, Guo Man, et al. Analysis and Discussion of the Load Test of Manually Digging Piles of Qingdao Jiaodong International Airport [J]. Mechanics in Engineering, 2023,45(4):765-776.
6. WANG Xiwu, PENG Jian, CAO Zhengcong, et al. Numerical Simulation and Regression Analysis of Undisturbed Soil Digged Foundation Considering Soil Resistance [J]. Engineering Journal of Wuhan University, 2008(S1).
7. Hao D, Chen R, Fan G. Ultimate Uplift Capacity of Transmission Tower Foundation in Undisturbed Excavated Soil[J]. Energy Procedia, 2012,17:1209-1216.
8. Yu Haijian. Research on the Interaction Between the Retaining Wall and the Body of Artificial Excavating Pile Under Vertical Load Together With the Contribution in Bearing Capacity of the retaining wall[D]. A Dissertation Submitted for the Degree of Master. Chang'an University, Xi'an, China, 2011.
9. Gao Bo. Study on the Evolution of Stress State of Artificial Digging Hole Pile Retaining Wall in Construction Process[D]. Thesis for Master Degree. Shandong University, Jinan, China, 2015.
10. Lv Hongying. Analysis of Uplift Bearing Capacity of Transmission Line Tower Excavated Enlarged Base Piles [D]. Thesis for Master Degree. Shandong University of Science and Technology, Qingdao, China, 2017.
11. Guo Yu, Qi Wenjing. Study on Vertical Load-Carrying Capacity of Post-Grouting Bored Piles [J]. Engineering and Test, 2024,64(03):50-53+92.
12. Men Qingbo,Qiao Jianwei. Field Tests Study on Post-Grouting Cast-in-Place Bored Piles in Soft Soil Area of Indonesia[J]. Geotechnical Engineering Technique, 2024,38(01):121-126.

13. Lu Pingzhen,Sun Hongwei. Test Analysis of Post-Grouting Improvement Coefficient for Cast-in-Situ Pile in Thick Sand Layers[J]. Geotechnical Engineering Technique, 2022,36(02):116-121.
14. Yang Xiaonan,Sun Huaijun. Effects on Plasticity Index of Cohesive Soil on Lateral Resistance of Post-Grouting for Cast-in-Situ Piles[J]. Investigation Engineering Technique,2023,(02):6-9.